DESIGN LOADS FOR THE KEEL OF A SAILING YACHT

Abstract. The paper describes experimental drop tests of a sailing yacht model down on to a calm water surface and reports results for the deceleration of the hull and for bending loads on the keel. Based on similarity laws, recommendations can be given for the design loads of full-scale yacht keels.

NOMENCLATURE

A_{LK}	Lateral area of keel
a_x, a_y, a_z	Components of the acceleration vector
B_{max}	Beam of the hull
B_{WL}	Beam of waterline
C_K	Keel fin section chord length
c_J	Torsion spring coefficient
E	Modulus of elasticity (Young's modulus)
e	Lever arm of lateral area of keel
g	Acceleration due to gravity
h	Drop height
h_D	Design head, bottom panel, ABS-rule
I	Second moment of area of keel fin
K_α, K_{pot}, K_Θ	Constants used for abbreviation
L_{OA}	Length overall
L_{WL}	Length of waterline
M	Bending moment of keel fin
m_1	Mass of hull (canoe body)
m_2	Mass of fin keel, including bulb (ballast)
$P_{BS,BASE}$	Base bottom pressure (ISO 12215-5)
r	Distance from common center of gravity
S	Length scale factor
s	Distance from keel-hull junction
T	Kinetic energy of the falling yacht
T_{max}	Maximum draft including keel
T_C	Draft of canoe body
t_K	Keel fin section thickness
V	Potential Energy of the falling yacht
v	Impact speed
w	Deflection by bending
x	Coordinate in fore and aft direction of yacht
y	Coordinate in transverse direction of yacht
z	Vertical coordinate, parallel to the mast
ζ	Vertical coordinate in earth fixed system
α	Angle of deflection
φ	Angle of heel
ρ_w	Density of water
ν	Poisson's number
∇	Volume displacement of hull and keel
Θ	Mass moment of inertia
ω	Angular frequency

1. INTRODUCTION

The structural design of a yacht is usually based on the scantling rules of one of the classification societies, which are recognized as proven industry standard, or lately on ISO 12215-5 [1]. These scantling rules are comprehensive for most parts of a sailing yacht, with one exception; there is a lack of data for the determination of the proper design loads of the keel-hull junction. This is astonishing, since the loss of the keel, leading to capsize is probably the most dangerous hazard in sailing craft structure. This is recognized in ISO 12215 by devoting an entire part to this subject, but the discussion is still ongoing and ISO 12215-9 exists only in draft version.

Reviewing the recommendations for keel design loads that are available [2, 3, 4, 5, 6], there might be different discussions of grounding scenarios, but for the transverse design load one must realize, that the assumptions are all based on the keel weight and the static momentum it exerts on the keel-hull junction at 90 degree heel. The draft of ISO 12215-9 also follows this approach. The rules only differ in the applied safety factor. An industry survey of 9 GRP sailing yachts [7] revealed a variation of the safety factor for the floor members between 1.9 and 21. ISO 12215-9 proposes a safety factor of 3. This wide variation indicates the existence of different load assumption methods throughout the industry. It is also questionable whether the maximum forces on a keel in a seaway depend only on the keel weight.

Coles [8] concludes from his investigations of marine accidents that the severest damage to a yacht occurs on her leeside when she is falling off a wave crest, hitting the solid water surface beneath. Following these findings, it seems necessary to investigate the water impact loads on the keel fin under such circumstances and compare these dynamic loads on the keel to the static approach of ISO 12215-9. Water impact loads on boats of yacht size, but without keel, have been investigated during the introduction of the free-fall lifeboat. Boef [9] provides an analysis where the added mass during impact is calculated using von Karman's two-dimensional approximation. This simplified approach cannot be adapted in this form to a hull with a keel. Faltinsen and Chezhian [10] report numerical and experimental results for a three-dimensional idealized body. The strong influences of the three-dimensionality and of the elastic response of the body are pointed out. A yacht consisting of a canoe body with an attached fin keel creates a much more complex flow field during impact than e.g. a lifeboat. A cavity between keel and hull formed during impact and the flexibility of the keel-hull joint might even increase this complexity. In [11] it is stated that "The model and full-scale measurement of slamming pressures are still the most reliable approaches in investigating the characteristics of impact loads …". Following this recommendation, fully instrumented model tests seem to be the best approach for the hull with keel. The need for a scale model

is obvious, since harsh tests that require the repeated drop of a sailing yacht from different heights down to the water surface cannot be conducted at full scale. The scaling laws that govern the design of the model are not trivial. The choice of parameters must be based on an analysis of the elastic properties of the keel-hull system.

2. DYNAMIC RESPONSE OF THE KEEL-HULL SYSTEM

The hull (canoe body) and the ballast keel have their own masses and moments of inertia and they are connected by a joint that is not rigid. As a consequence, the hull and keel can oscillate in angular motions and will exhibit resonance effects near the natural frequency. The forces on the keel during a drop test depend therefore not only on geometry and impact speed but also on the impact time in relation to the natural period of the system. It is possible to calculate the natural frequency from first principles. Figure 1 shows the motions of the system in the transverse plane.

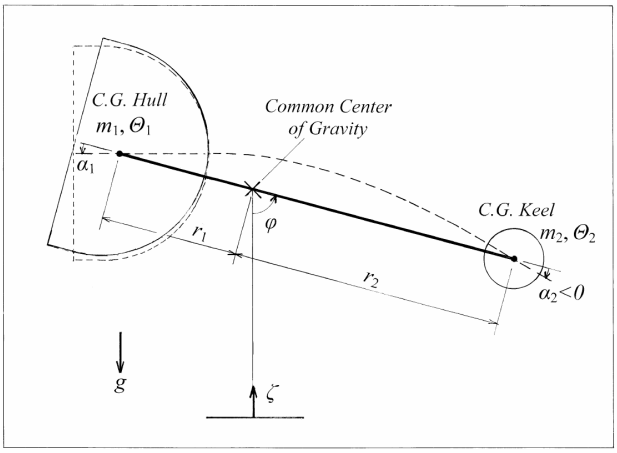

Figure 1. Kinematics during free fall

During free fall hull and keel can oscillate freely around their common center of gravity. In addition, the keel fin can bend dynamically which will lead to a rotation of keel and hull around their individual centers of gravity. A straight line connects the centers of hull, keel and their common center. Let φ be the heel angle at which this line tilts relative to the vertical direction and α_1 and α_2 be the angles at which the masses of hull and keel move relatively to the connection line. The vertical position of the centre of gravity is denoted ζ. The equations of motion will be derived by using Lagrange's equations:

$$\frac{d}{dt}\left(\frac{\partial T}{\partial \dot{q}_j}\right)-\frac{\partial T}{\partial q_j}-\frac{\partial V}{\partial q_j}=0 \tag{1}$$

The kinetic energy T of the system is:

$$T=\tfrac{1}{2}\cdot m_1\cdot r_1\cdot\dot{\varphi}^2\cdot(r_1+r_2)+\tfrac{1}{2}\cdot m_1\cdot\frac{r_1+r_2}{r_2}\cdot\dot{\zeta}^2 + \tfrac{1}{2}\cdot\Theta_1\cdot(\dot{\alpha}_1+\dot{\varphi})^2+\tfrac{1}{2}\cdot\Theta_2\cdot(\dot{\alpha}_2+\dot{\varphi})^2 \tag{2}$$

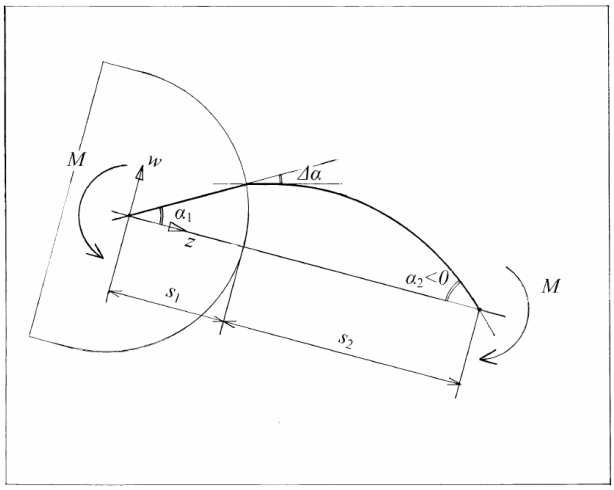

Figure 2. Bending moments and deflections at the keel

The potential energy V follows from the work against the spring force at the keel. Beam theory is applied as shown in figure 2. The hull is considered as rigid, the keel fin is a flexible and massless beam and the bending moment is constant along the beam. The elastic joint between hull and keel is modeled by a jump in α that is proportional to the bending moment.

$$\Delta\alpha=-c_J\cdot M \tag{3}$$

This is Hooke's law for a torsion spring. The spring constant c_J is either calculated from the stiffness of the floors or measured in a static test. Inside the hull we know the deflection:

$$w=\alpha_1\cdot z \tag{4}$$

Outside of the hull the second derivative of the deflection for a wide beam is

$$w''=-\frac{M\cdot(1-\nu^2)}{E\cdot I}=\frac{d\alpha}{dz} \tag{5}$$

At $z = 0$ we know $w = 0$ and $\alpha = \alpha_1$ and at $z = (s_1+s_2)$ we know $w = 0$ and $\alpha = \alpha_2$. Combining these boundary values with equations (3) to (5) yields:

$$\frac{\alpha_2}{\alpha_1}=1-K_\alpha \tag{6}$$

where $$K_\alpha=\frac{s_1+s_2}{s_2}\cdot\frac{s_2/B+c_J}{\frac{1}{2}\cdot s_2/B+c_J}$$

and $$B=\frac{E\cdot I}{1-\nu^2}$$

finally for the bending moment M in the beam:

$$M \cdot \alpha_1 \cdot K_\alpha = K_{pot} \cdot \alpha_1^{\,2} \tag{7}$$

with $$K_{pot} = \frac{(s_1 + s_2)^2}{s_2^{\,2}} \cdot \frac{s_2/B + c_J}{\left(\frac{1}{2} \cdot s_2/B + c_J\right)^2}$$

The potential energy V for linear bending is calculated from the bending work at both ends of the beam plus the gravitational potential:

$$\begin{aligned} V &= \tfrac{1}{2} \cdot (M \cdot \alpha_1 - M \cdot \alpha_2) + (m_1 + m_2) \cdot g \cdot \zeta \\ &= \tfrac{1}{2} \cdot K_{pot} \cdot \alpha_1^{\,2} + (m_1 + m_2) \cdot g \cdot \zeta \end{aligned} \tag{8}$$

The q_j in Lagrange's equations are the generalized coordinates φ, α_1 and ζ. Damping forces will be neglected. For $q_j = \zeta$ we get from equations (1), (2) and (8):

$$\ddot{\zeta} + g = 0 \tag{9}$$

for $q_j = \varphi$ we get:

$$\begin{aligned} &m_1 \cdot r_1 \cdot (r_1 + r_2) \cdot \ddot{\varphi} + \\ &\Theta_1 \cdot (\ddot{\alpha}_1 + \ddot{\varphi}) + \Theta_2 \cdot [(1 - K_\alpha) \cdot \ddot{\alpha}_1 + \ddot{\varphi}] = 0 \end{aligned} \tag{10}$$

and for $q_j = \alpha_1$

$$\begin{aligned} &\Theta_1 \cdot (\ddot{\alpha}_1 + \ddot{\varphi}) + \\ &\Theta_2 \cdot [(1 - K_\alpha) \cdot \ddot{\alpha}_1 + \ddot{\varphi}] \cdot (1 - K_\alpha) + K_{pot} \cdot \alpha_1 = 0 \end{aligned} \tag{11}$$

combining equations (10) and (11) finally gives the homogenous differential equation of motion without damping:

$$\ddot{\alpha}_1 \cdot K_\Theta + \alpha_1 \cdot K_{pot} = 0 \tag{12}$$

with

$$K_\Theta = \Theta_1 + \Theta_2 \cdot (1 - K_\alpha)^2 - \frac{[\Theta_1 + \Theta_2 \cdot (1 - K_\alpha)]^2}{\Theta_1 + \Theta_2 + m_1 \cdot r_1 \cdot (r_1 + r_2)}$$

The solution of (12) is the harmonic oscillation of α with the natural frequency ω, where

$$\omega^2 = \frac{K_{pot}}{K_\Theta} \tag{13}$$

This frequency is the characteristic parameter for the elastic properties of the model. During the free fall the keel will oscillate with this frequency.

3. MODEL DESIGN

The model must be similar to the full size yacht in all parameters that influence the forces and accelerations during water impact. The similarity requirements can be divided into three categories.

3.1 Geometric similarity

A constant factor S is applied to the outer dimensions of the yacht to get the scaled dimensions of the model. Table 1 lists the principal dimensions, areas and volumes are scaled with the 2nd and 3rd power of the length scale factor S.

L_{OA}	10.31 m
L_{WL}	9.20 m
B_{max}	2.70 m
B_{WL}	2.42 m
T_{max}	2.11 m
T_C	0.60 m
m_1 without mast	3791 kg
Θ_1 without mast	1189 kg·m^2
m_2	1226 kg
A_{LK}	1.53 m^2
mast length	14.4 m

Table 1. Main dimensions of model, scaled to full size, S = 9

3.2 Hydromechanic similarity

The hydrostatic similarity is fulfilled if the model is loaded to the design waterline. The tests were conducted in fresh water.

The hydrodynamic similarity depends on Reynolds and Froude number. A meaningful definition of the Froude number for a vertical drop could be

$$Fn = \frac{v}{\sqrt{g \cdot T_{\max}}}$$

where v is the vertical speed immediately before water impact. After a free fall this speed is

$$v = \sqrt{2 \cdot g \cdot h} \tag{14}$$

This implies that the model test will be conducted at the correct Froude number if the drop height is scaled from full size by division with the scaling factor S. It also means that the Reynolds number cannot be kept constant. This does not introduce an error since during initial impact, where the high loads occur, frictional forces are negligible. Moghisi and Squire [12] have shown that above a Reynolds number of 1 the impact force is independent of the Reynolds number. The following tests are conducted at Re > 33000 (in the definition of [12]).

3.3 Hydroelastic similarity

Similarity in the elastic response of the keel will be achieved if the deflections change with the length scale S and the natural periods of oscillations follow the time scale $\sqrt{S}$. The similarity of deflections requires $\Delta\alpha$ to remain constant and according to equation (3) c_J to be proportional to $1/M$, i.e. the scaling factor of c_J is $1/S^4$. On the other hand, if the floors were treated as a beam and

the dimensions scaled geometrically multiplying them by S, the deflection angle of the floors divided by the moment would follow $1/S^3$, material and the modulus of elasticity remaining unchanged. This results in the floor section of the model being too stiff if scaled geometrically from the full size yacht. Therefore the model for the drop tests has in the keel area no floors but a sandwich bottom instead. This reduces the stiffness and gives a high safety against breaking, which is important for severe testing. The stiffness of the floors in a full size yacht varies, depending on the scantling rules that are used.

Parameter	**Scaling factor**	**Model, scaled to full size**	**full size floors based on [2]**	**full size floors based on [5]**
C_K	S	0.95 m	0.95 m	
t_K	S	0.045 m	typical yacht 0.12 m	
material keel fin		aluminum	cast iron	
ballast bulb		steel	lead	
Θ_2	S^5	172 kg·m^2	268 kg·m^2	
floor height	-	sandwich	4 x 0.16m	3 x 0.256m
c_J [1/Nm]	$1/S^4$	measured $1.83 \cdot 10^{-7}$	calculated $5.67 \cdot 10^{-7}$	calculated $1.63 \cdot 10^{-7}$
natural frequency	$1/\sqrt{S}$	14.9 Hz	10.4 Hz	18.0 Hz
static safety factor at 90 deg. heel		38	5.0	9.1

Table 2. Parameters relevant for elastic properties of keel

In table 2 the designs for a GRP hull according to Larsson [2] and Gerr [5] are shown for comparison. For the design of the model keel a few compromises hat to be accepted. To get a significant strain in the keel fin that can be measured with a strain gauge, a thin blade from a homogenous material with a low modulus of elasticity had to be used. An aluminum plate was chosen with a steel bulb at the bottom. With appropriate dimensions, it was possible to fulfill the requirements of similar deflections and similar natural frequency, see table 2 for results. The model values are between the two scantling rules.

The hull shell outside of the keel area is made of single-skin fiberglass. The thickness of the laminate can be chosen either for similar deflection or for similar natural frequency, see Manganelli et al. [13] for a detailed discussion. In table 3 both dimensions are given. Since the planned tests are only focused on the keel response, the skin thickness of the hull is modeled close enough to a typical yacht.

bottom skin thickness according to ABS [2]	11.1 mm
bottom skin thickness according to [5]	7.8 mm
model skin thickness scaled with $S^{4/3}$ for similar deflection	9.4 mm
model skin thickness scaled with $S^{3/2}$ for similar natural frequency	13.5 mm

Table 3. Choice of hull laminate thickness

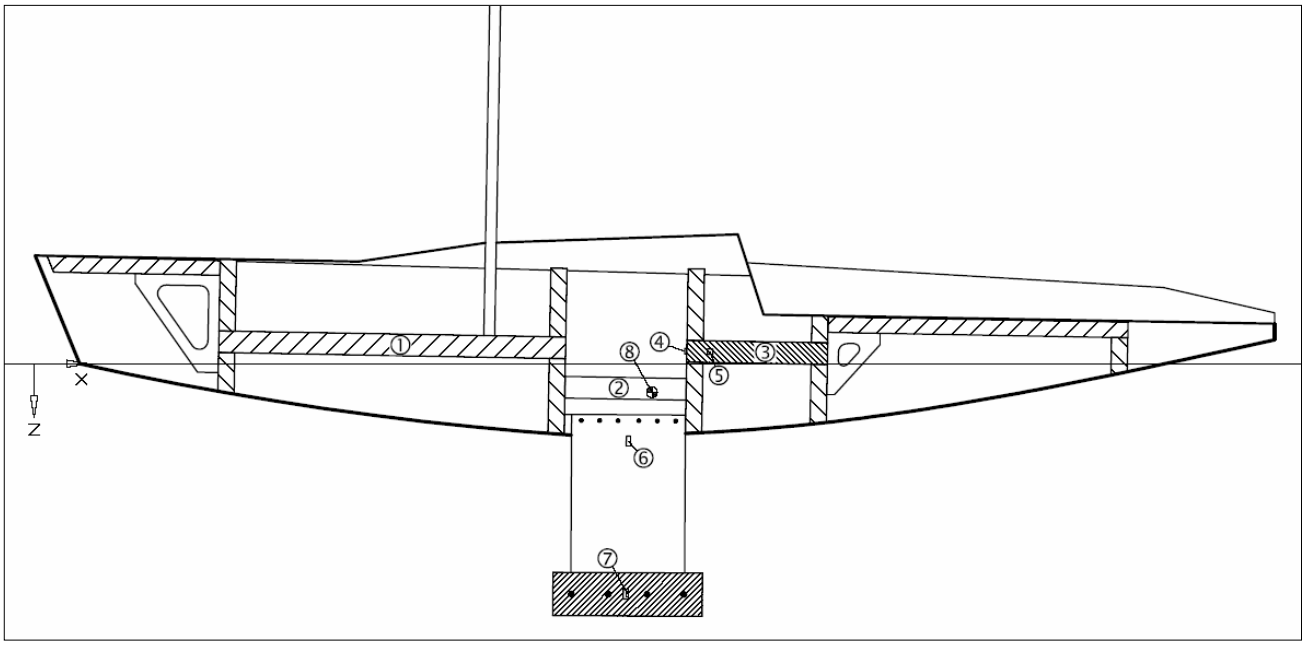

Figure 3. Longitudinal section of model

① wooden framework
② removable internal ballast, 2 in parallel
③ fixed internal ballast
④ accelerometer, *y*- and *z*-direction
⑤ accelerometer, *x*-direction
⑥ strain gauge
⑦ accelerometer, φ-direction
⑧ common center of gravity

During the water impact there is the chance of air being entrapped under the hull, reducing the impact forces through a cushioning effect. Takagi and Dobashi [14] demonstrate that this effect cannot be scaled properly in a model test at ambient air pressure. Based on a numerical simulation Bereznitski [15] comes to the conclusion that air cushioning effects can be neglected, if the angle between the water surface and the hull panel is larger than 5 degrees. In this case the air escapes during impact. The following tests will show that the large forces, determining the design load, will occur at heel angles around 60 degrees when there are no flat surfaces hitting the water and air can easily escape. Entrapped air is therefore not considered to become a problem in the scaling of the test results.

3.4 Internal structure

The GRP hull shell is supported by a wooden framework that consists of five transverse frames and a connecting backbone. To avoid additional stiffening of the skin no longitudinal stringers are installed. The deck is glued on to the hull flange. The result of this design is a very low structural weight requiring additional internal ballast to reach the desired displacement. The internal ballast is formed out of three steel bars that are tightly bolted on to the frames. Two of them are removable and can be added to the keel bulb to change the ballast ratio of the model. A longitudinal section of the model is shown in figure 3 and a photograph of the inside of the hull can be seen in figure 4.

Figure 4. Internal hull structure

4. MODEL INSTRUMENTATION

The required quantities from the water impact test are the accelerations at the center of gravity of the model in all three axes, the rotation around the center of gravity and the bending moment at the keel root. All these parameters need to be measured as functions over time. The model will be dropped from rest and in a horizontal attitude of the fore and aft axis. It is therefore sufficient to measure the rotation only in the transverse plane.

Two accelerometers are cemented to the fixed steel bar, close to the center of gravity. One bi-directional accelerometer measures the values in *y*- and *z*-direction and the second accelerometer measures the *x*-direction. Figure 5 is a photograph of the arrangement. The accelerometer for the rotation is placed inside the keel bulb and it measures the acceleration vertical to the keel fin. The positions of the accelerometers can also be taken from the drawing in figure 3.

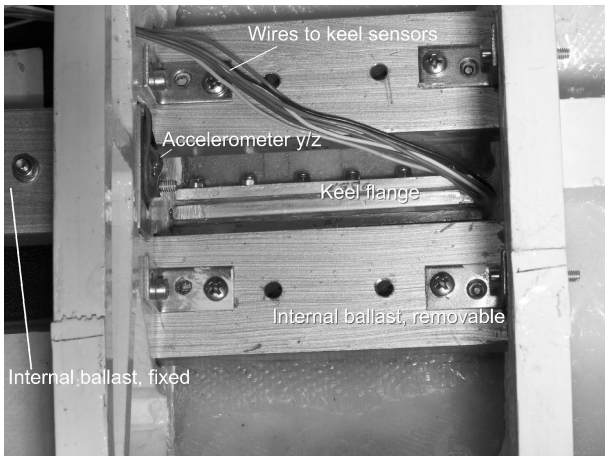

Figure 5. Downward view into the hull

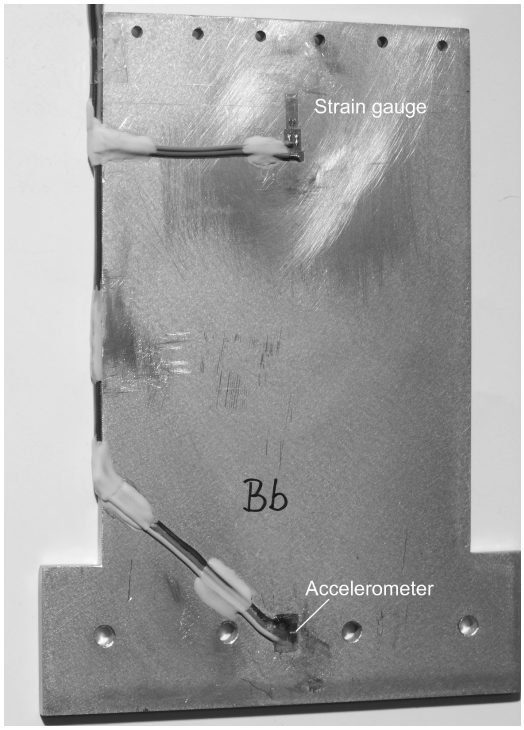

Figure 6. Aluminum plate as keel fin

The bending moment at the keel root is measured by two strain gauges, placed on the sides of the keel fin. The en-

capsulated gauges have a length of 5 mm and a polyimide backing. They are connected in a half bridge, which doubles the output signal. Figure 6 shows the gauge on the port side. The gauge on starboard is mirror imaged. Prior to entering the water, gauges and wiring are covered with putty to protect them from humidity (figure 7). The signals of all accelerometers and strain gauges, including a sense lead for compensation, are transmitted from the model to the shore via a 10-core cable of 7 meter length. The cable is unshielded, therefore flexible and has a weight of only 0.072 kg/m. This allows it to neglect the influence of the cable on the model movement during the drop. At the shore, the signals are amplified in a 16 bit A/D-converter and stored in a laptop computer. The sampling rate is 1 kHz. The resolution and accuracy of the measurements can be summarized as follows:

strain gauge	bending moment
offset	compensated at start of test
offset drift	-1 kNm (full scale yacht) at end of test
conversion factor	static calibration
temperature depend.	compensated, < 0.2%
resolution	8 Nm for full scale yacht
accelerometer	all directions
nonlinearity	0.2 %
offset and sensitivity	calibrated in software for each drop
resolution	0.004 g

The accelerometers measure the force per mass. They cannot distinguish between a force due to an acceleration of the body and the force from the gravitational field. The indicated value is the sum of both. Speeds, distances and angles are calculated from the accelerations by integration of the time-functions. The signal of the strain gauges is converted to the bending moment using the static calibration curve and scaled to full size proportional to the 4^{th} power of the length scale.

Figure 7. Model ready for drop test

5. TEST IMPLEMENTATION

The tests took place on a landing stage at Lake Constance, on calm days early in the morning, when the waves on the water surface were still small. The water was more than 5 meters deep, which is sufficient for a model of 1 meter length. The model was suspended from three strings, attached to bow, stern and ballast bulb. The strings were connected to a wire that ran over a pulley resting at least 1.6 meters above the water surface. The model was steadied at a predetermined distance above the water and then rapidly released.

5.1 Sequence of events

The model goes typically through several different phases during the fall and water impact. An understanding of the kinematics is vital for the assessment of the damage risk. Figures 8, 9 and 10 show the sequence of the events. At the time t = 0 ms the model hangs at rest above the water, the accelerometer *y/z* indicates 1g. During the following free fall the model is almost weightless and the accelerometer measures 0g. At t = 350 ms the ballast bulb is shortly before impact. Attitude and heel angle changed very little during the free fall. The third picture in figure 9 at t = 383 ms depicts the moment, when the ballast bulb is in the water. The acceleration is 0.5g, but more important, the impact force on the bulb creates a rotation of the model around its center of

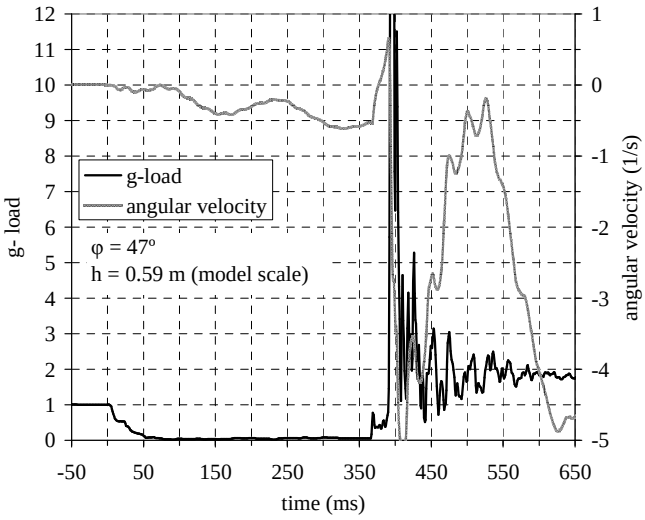

Figure 8. Resultant force measured by accelerometer *y/z* and angular velocity measured by the accelerometer in the keel, all at model scale

mass that increases the heel angle. On the photograph it can be seen that the top part of the mast is relative to the bottom part slightly bent to port because of this rotation. In figure 8 the angular velocity at t = 383 ms is >0 which also indicates that the heel angle φ increases. Shortly after, at t = 400 ms, the starboard topside hits the water creating the highest g-force of the drop, followed by a violent rotation in the uprighting direction, decreasing φ. The fourth picture in figure 9 captures this moment of strongly negative angular velocity at t = 416 ms. Corres-

Figure 9. Time sequence of drop test

pondingly the top part of the mast is bent to starboard. The boat continues its righting motion but its angular velocity reduces almost to 0 at t = 500 ms. The mast seems to be only loosely coupled to the boat and continues swinging to port, as can be seen in the last picture of figure 9 at t = 550 ms.

The bending of the keel is depicted in figure 10. The maximum moment coincides with the maximum acceleration exciting strong keel vibrations.

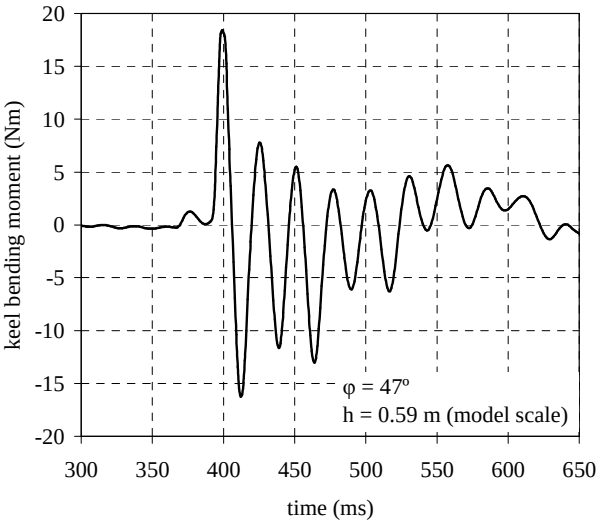

Figure 10. Bending moment at the keel root at model scale

5.2 Natural frequency

It is of interest to verify the natural frequency that was calculated in chapter 2. experimentally. The phase of the free fall can be used for this measurement. When the model is supported by the three strings at bow, stern and bulb, the keel is bent downward by its weight. When the model is released, the keel straightens and swings back and forth at its natural frequency without interference from outside. Figure 11 presents the time series of the strain gauge during the free fall. The natural frequency for the model without mast is 44.6 Hz, which coincides exactly with the calculated value. The frequency for the model with mast is only marginally higher at 44.9 Hz. If the mast were inflexible and solidly fixed to the model,

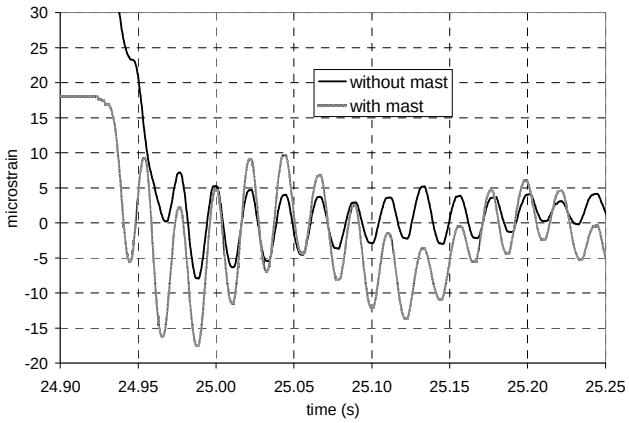

Figure 11. Strain gauge signal during free fall

the natural frequency would be going down to 29 Hz. The experimental value proves that the mast can be regarded as detached from the model and the model parameters without mast can be used for calculations. The scaled value of the frequency for the full size yacht is 14.9 Hz. The natural frequency of the keel in the water is lower than in air because of the added mass. A value of 38.7 Hz can be read from figure 10.

6. RESULTS

The tests comprised a variation of the parameters

- drop height
- heel angle
- with/without mast
- ballast ratio
- length/displacement ratio

	Basic w/mast	No mast	Light displace-ment	High Ballast
$L_{WL}/\nabla^{1/3}$	5.35	5.37	5.68	5.35
m_2/∇	0.239	0.244	0.316	0.482
conventio-nal keel design moment	71.6 kNm	71.6 kNm	71.6 kNm	152 kNm

Table 4. Tested configurations of the model

See table 4. The keel design moment for the full size yacht according to [2] is given for information. It would be used if the yacht were conventionally designed. It is the static keel moment at 90 degrees heel, multiplied with a safety factor of 5.

6.1 Bending moment

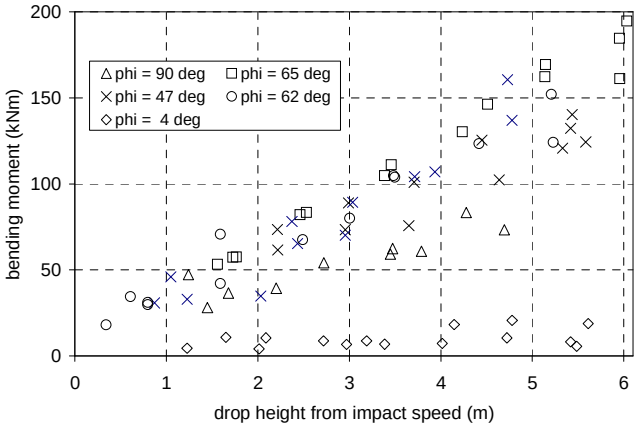

Figure 12. Bending moment at full scale, basic w/mast

The drop height and the heel angle are the parameters of major influence on the bending moment at the keel root. Figure 12 shows the results of the basic model with mast. The drop height is calculated from the measured impact speed using equation 14. A linear trend of the bending moment over drop height can be noticed. The highest loads occur at around 62 to 65 degrees of heel, when the

keel and the topsides hit the water simultaneously. The large scatter of the data is not caused by a measurement error but rather by an almost chaotic behavior of the system. Small wavelets on the surface can determine whether the keel or the topsides hit the water first, causing opposite values of the initial rotation. There were incidences when an oscillating rotation led to a second impact of the keel exceeding the forces of the first impact. Like in chaotic systems, small differences in the initial conditions can lead to a totally different sequence of events with a considerably different result.

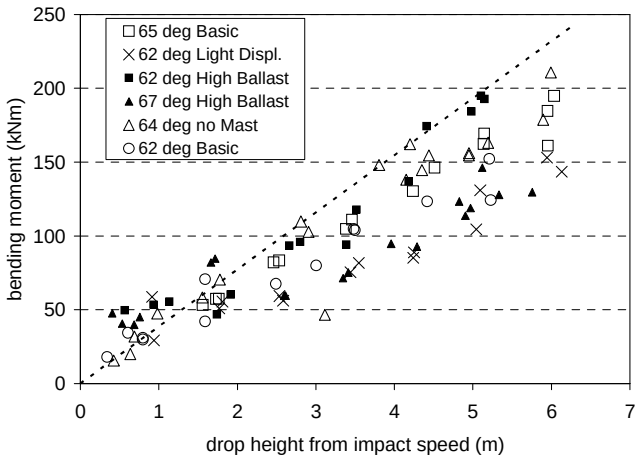

Figure 13. Bending moment at full scale

The influence of the different model configurations at critical heeling angles is compared in figure 13. Looking at 62 degree heel, the high ballast ratio increases the bending moment slightly and the light displacement reduces it, compared to the basic configuration. On the other hand, increasing the heeling angle for the high ballast ratio from 62 to 67 degrees reduces the bending moment below the basic version. One must therefore conclude that the ballast weight is not a major determining factor for the bending moment. The highest bending moments actually occur with the model without mast. It seems to be useful to define a curve of maximum bending moments in form of an envelop around the measurement points. The dotted line in figure 13 is such a curve of maximum bending moment for the given lateral area of the keel. The fact that at very small impact speeds the measured moments are lying above the line is due to the righting movement. Even without vertical speed, the rotation exerts a bending moment on the keel. This is especially true for the high ballast ratio with the large righting moment. The equation for the dotted line is:

$$M = 3.25 \cdot \rho_w \cdot g \cdot h \cdot A_{LK} \cdot e \qquad (15)$$

where e is the distance from the geometric center of the lateral area of the keel to the root of the keel. This equation might have only a limited validity, but it can be used for typical yachts, as long as the actual form of the keel is not too different from the tested versions. It is interesting to compare the conventional design moments according to [2] of 71.6 and 152.3 kNm, as given in table 4, to the measured bending moment. Equation (15) indicates corresponding drop heights of 1.85m and 3.94m for the conventional design moments. The smaller value for the yacht with the lower ballast ratio might result in a design of insufficient strength.

6.2 Accelerations

The accelerations during impact need to be known, because the persons on board must be able to survive the impact without serious injury. If the accelerations are not survivable, the keel may also fail. The forces acting on a person in the boat depend on his or her position relative to the center of mass. The larger the radial distance is, the higher is the additional acceleration caused by the rotation. A person on the siderail can therefore suffer much higher accelerations than a person near the center of mass would experience. The values measured by the *y/z*-accelerometer are taken as representative, because the position in the middle of the cabin is a typical location for a person that one would consider safe during a storm.

During the tests high acceleration peaks up to 27g could be observed. From automobile crash research it is known that not only the height of the acceleration peak but also its duration is important for the assessment of the injury risk. A head injury criterion (HIC) is defined in [16]:

$$HIC_{15} = Max\left[0.015s \cdot \left(\tfrac{1}{0.015s} \cdot \int_t^{t+0.015s} a_{res} \cdot dt \right)^{2.5} \right]$$

where

$$a_{res} = \sqrt{a_x^{\,2} + a_y^{\,2} + a_z^{\,2}}$$

in analogy to this expression an effective acceleration a_{eff} is defined for the water impact tests:

$$a_{eff} = MAX\left(\tfrac{1}{0.015s} \cdot \int_t^{t+0.015s} a_{res} \cdot dt \right)$$

When calculating a_{eff} the time intervals need to be multiplied by the time scale $\sqrt{S}$. An interval of 0.015 seconds at full scale is equivalent to 0.005 seconds at model scale. Figure 14 summarizes the effective accelerations for all test results. At zero impact speed, the accelerometer indicates 1g because of the gravitation force. Again, it can be seen that heel angle and drop height have the largest influence. There seems to be a limiting curve that will not be surpassed by the acceleration values. The line in figure 14 follows the equation:

$$a_{eff} = MAX\left\langle 5.45 \cdot h^{0.8}, 1 \right\rangle \qquad (16)$$

The maximum effective acceleration during all tests was 23.2g. This value measured over a time interval of 15 ms at the head of a crash test dummy resulting in a HIC of only 39 would classify the impact as one of minor injury risk in automobile crash tests. However, this is valid only for occupants wearing seat belts and additionally protected by airbags. In the cabin of a yacht a person will be thrown against the wall or even against sharp edges, experiencing much higher g-loads during this later impact

between person and yacht. Useful information about the injury risk under such circumstances can be gathered from civil aviation accident reports. Maximum allowed g-load for a passenger aircraft during normal flight maneuvers is +2.5g vertical. There are numerous reports about injuries, like broken bones and ribs, of persons who did not have their seat belts fastened or of crew standing in the galley during maneuvers producing g-loads of 2g or less [17]. If a limit of 2.5g is applied to the water impact, a drop height of 0.4m results from figure 14. With an unfavorable heel angle, this is sufficient to produce the g-load that can seriously injure a person sitting or standing in the cabin.

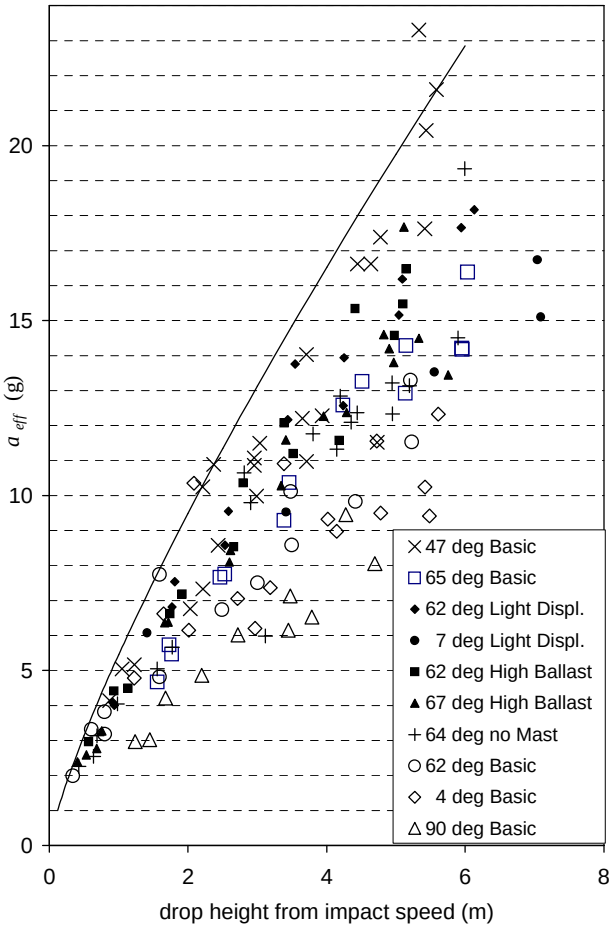

Figure 14. Effective acceleration at full scale

6.3 Design drop height

The choice of the drop height for the determination of the design load of the keel on the basis of the measured accelerations is obviously debatable. An alternative approach could ask for the maximum height and steepness of a breaking wave during a storm to calculate the drop height from the trajectory of the falling yacht. Chanson and Lee have conducted experiments in a wave flume [18] and found out, that the free falling plunging jet impacts the downstream water surface always above the still water level. If the yacht is not moving faster than the surrounding water, she can also not fall beyond this level. Therefore we can take the crest height above the mean sea level as the maximum drop height. The crest height of an individual wave depends on the significant wave height and the duration of the storm, i.e. the probability of encountering an extreme wave.

Such an encounter is described by Bertotti and Cavaleri [19]. On February 14, 2005 the passenger ship "Voyager" was hit by a breaking wave in the Mediterranean sea during a severe but not unusual mistral storm. The wave broke the windows on the bridge deck, flooded the electric controls and caused the engines to stop for several hours. Through a detailed analysis of the available data, Bertotti et al. arrived at a significant wave height between 8 and 10m for the time of the incident. The crest height of the damaging wave was estimated at 14m and a probability of encounter of once every 20 hours. Applying this situation to a sailing yacht would require a design drop height of 14m for a storm with a significant wave height of 10m. An even higher significant wave height of 20m is proposed by Smith [20] to be taken as the basis of all design criteria. He concluded this from a risk analysis for large commercial ships. Since sailing yachts tend to avoid storm seasons and can stay in harbor to wait for better weather, it seems sufficient to assume a maximum wave height of not more than 10m for the design of blue water cruising yachts.

An even different method to determine the design drop height is the comparison with the panel design of the hull. The keel junction does not have to be stronger than the hull skin. When following the ABS-rule [2] a design head is calculated, which is used to determine the maximum load on the bottom panel and the required skin thickness. For the yacht as described in table 1 this design head amounts to 56.4 kN/m^2. ISO 12215-5 [1] would give a slightly lower value of 51.5 kN/m^2 for base bottom pressure. Experiments that correlate impact pressures to a drop height are rare. The experimentally measured pressure is an average value calculated from the force on the panel divided by the projected area. The average pressure depends strongly on the size of the panel area, therefore the panel size in the experiment must be comparable to the panel size of the yacht. Useful experiments are reported in [10]. The forces are measured on a central section of the model that extends over a length of 20% of the total length. The measured pressure values compare to the design pressure and are directly proportional to the drop height. Solving for drop height yields:

$$h = 0.36 \cdot \frac{P_{BS,BASE}}{\rho_w \cdot g} \qquad (17)$$

With this relationship, a drop height of 2.1m would follow from the ABS-design head for the yacht of table 1.

7. CONCLUSION & RECOMMENDATIONS

The reported test results show that a design of the keel-hull junction solely dependent on the keel weight is not sufficient and might result in a structural design that is too weak. A design drop height should be determined in correspondence with the design head that was chosen for

the bottom panels of the yacht based on the scantling rules of the classification society. Equation (17) can be used until better test results become available. With the input of the design drop height equation (15) gives the design keel bending moment. This design moment should be used in addition to the conventional static keel moment for the dimensioning of the keel-hull junction. Figure 14 gives the accelerations that one must expect for the given design drop height. In most cases this will require the use of some kind of restraint system for the persons on board to survive the impact without injury. This approach seems to be sufficient for normal recreational sailing. For serious blue water cruising, including delivery trips without restrictions during all seasons, when safety is more important than boat speed, one should think about a much higher design drop height. A value of 10 meters for all hull scantlings seems to be an appropriate starting point for the discussion. This would double the structural weight of the boat but increase significantly the chance to survive severe weather. In parallel one must consider that such an increase in boat strength makes only sense if it is accompanied by the installation and usage of seatbelts like in passenger cars.

8. ACKNOWLEDGEMENTS

The CANSAS test equipment was provided and programmed by Laszlo Panghy from ZF Getriebe GmbH in Kressbronn, Germany. His support is gratefully acknowledged.

9. REFERENCES

1. TC188, Small craft., ISO 122215-5, *www.iso.org*, 2008
2. LARSSON, L., ELIASSON, R. E., Principles of Yacht Design, *Adlard Coles, London GB*, 1994
3. Committee V.8, Sailing Yacht Design, *17th International Ship and Offshore Structures Congress, Seoul Korea*, 2009
4. CLAUGHTON, WELLICOME, SHENOI, Sailing Yacht Design, Part1 Theory & Part 2 Practice, *University of Southampton GB*, 2006
5. GERR, D., Boat Strength, *International Marine, Camden USA*, 2000
6. GERMANISCHER LLOYD, Rules for Classification and Construction, chapter I-3-3, *Hamburg D*, 2003
7. LOSCOMBE, R., International Small Craft Industry Consultation and Validation Study, *ISO/DIS-12215-9, eba / ISAF / RYA*, 2009
8. COLES, K. A., Heavy Weather Sailing, *Adlard Coles, London GB*, 1980
9. BOEF, W. J. C., Launch and Impact of Free-Fall Lifeboats. Part II and II, *Ocean Engineering, 19, 119-159*, 1992
10. FALTINSEN, O. M. and CHEZHIAN, M., A Generalized Wagner Method for Three-Dimensional Slamming, *J. Of Ship research, 49, 279-287*, 2005
11. Committee V.7, Impulsive Pressure Loading and Response Assessment, *17th International Ship and Offshore Structures Congress, Seoul Korea*, 2009
12. MOGHISI, M., SQUIRE, P. T., An experimental investigation of the initial force of impact on a sphere striking a liquid surface, *J. of Fluid Mechanics, Vol. 108, 133-146*, 1981
13. MANGANELLI, P., WAGEMAKERS, B., WILSON, P. A., Investigation of Slamming Loads Using Slam Patches on a Scale Model of an OPEN60 Class Yacht, *Intern. J. of small Craft Technology, 15(1), 35-42*, 2003
14. TAKAGI, K., DOBASHI, J., Influence of Trapped Air on the Slamming of a Ship, *Journal of Ship Research, 47, 187-193*, 2003
15. BEREZNITSKI, A., Local hydroelastic response of ship structures under impact loads from water (slamming), *PhD Thesis, Delft University of Technology, NL*, 2003
16. Nat.'l Highway Traffic Safety Admin., Federal Motor Vehicle Safety Standards, *49CFR571.208, USA*, 2000
17. National Transportation Safety Board, Aviation accident reports, *www.ntsb.gov, USA*
18. CHANSON, H., LEE, J.F., Plunging Jet Characteristics of Plunging Breakers, *Coastal Engineering, 31, 125-141*, 1997
19. BERTOTTI, L., CAVALERI, L., The Predictability of the 'VOYAGER' Accident, *Natural Hazards and Earth System Sciences, 8, 533-537*, 2008
20. SMITH, C. B., Extreme Waves and Ship Design, *10th Internat'l Symp. on Practical Design of Ships and other Floating Structures, Houston TX, USA*, 2007